

Imaging characteristics of spindle cell lipoma and its variants

Alla Khashper · Jiamin Zheng · Ayoub Nahal ·
Federico Discepolo

Received: 15 June 2013 / Revised: 17 January 2014 / Accepted: 21 January 2014 / Published online: 20 February 2014
© ISS 2014

Abstract A spindle cell lipoma (SCL) is a relatively common tumor that can be challenging to the radiologist, pathologist, or surgeon to diagnose, particularly when internal fat content is scant or absent. Although these lesions may be found at various locations, the typical presentation for this lesion is a well-circumscribed and non-aggressive subcutaneous mass in the posterior neck presenting in a middle-aged to elderly man. In this article, the typical and atypical imaging characteristics of a spindle cell lipoma (SCL) will be reviewed. Knowledge of the common imaging and pathologic features of SCLs can help suggest the diagnosis and guide patient management.

Keywords Spindle cell lipoma · Lipomatous tumor · Fat-containing lesion · Non-adipose component · Soft tissue

Introduction

The vast majority of subcutaneous tumors are benign, while malignant subcutaneous lesions are rare [1]. Lipomas account for nearly half of all soft tissue tumors and they represent by

far the most common subcutaneous masses [2, 3]; they are usually of little clinical concern. The World Health Organization (WHO) classifies benign lipomatous lesions into nine distinct entities: a lipoma, lipomatosis, lipomatosis of a nerve, lipoblastoma, angioliipoma, myoliipoma of soft tissue, chondroid lipoma, spindle cell/pleomorphic lipoma, and hibernoma [3, 4]. They are generally easily recognized on computed tomography (CT) and magnetic resonance imaging (MRI) due to their characteristic fatty content.

Spindle cell lipomas (SCLs) are benign lesions that are usually located in the subcutaneous tissues of the shoulder, neck, and upper back. They have a benign clinical course without local recurrence after excision [5, 6]. In many cases, spindle cell lipomas are treated surgically without imaging due to their typical clinical presentation and localization.

A lipoma with a spindle cell subtype can represent a diagnostic challenge to radiologists, pathologists, and surgeons given its frequent presentation as a lesion containing little or no macroscopic or microscopic fat. SCLs can also exhibit intramuscular extension. In the presence of these features, imaging-based diagnosis of SCLs can be extremely difficult given the radiographic overlap and similarity with liposarcoma, schwannoma, or other soft tissue tumors. In such cases, a patient can undergo a wide excision of tumor. This unnecessarily aggressive surgery can result in increased postoperative morbidity.

The aim of this review is to illustrate imaging features of spindle cell lipomas with and without fat content as well as to provide differential diagnostic possibilities for these lesions. Correct clinical, imaging, and pathology-based diagnosis of SCLs can help the clinician plan future surgical management.

Materials and methods

The Institutional Review Board at the McGill University Health Centre (Montreal, Quebec, Canada) approved this

A. Khashper (✉) · J. Zheng
Department of Radiology, McGill University Health Centre, 1650
Cedar Avenue, Montreal, QC H3G 1A4, Canada
e-mail: khashper@yahoo.com

J. Zheng
e-mail: jjajia08@gmail.com

A. Nahal
Department of Pathology, McGill University Health Centre, 1650
Cedar Avenue, Montreal, QC H3G 1A4, Canada
e-mail: ayoub.nahal@muhc.mcgill.ca

F. Discepolo
Department of Radiology, Jewish General Hospital, 3755 Cote
Sainte Catherine Road, Montreal, QC H4R 3H7, Canada
e-mail: federicodiscepolo@hotmail.com

study. Using a retrospective design, cases of spindle cell lipomas (SCLs) were extracted from our pathology database between 2006 and 2013. In total, 36 cases of SCLs were isolated, 19 of which had cross-sectional imaging including seven patients who were imaged with ultrasound (US), nine with computed tomography (CT), ten with magnetic resonance imaging (MRI), and three with positron emission tomography CT (PET-CT). Ultrasound exams were performed on Toshiba Aplio 3000 scanners using high-frequency matrix linear array and/or curved large field of view transducers. CT scans were acquired either on 16- or 64-slice GE Health Systems scanners. MRI was performed using a 1.5-Tesla GE Medical Systems scanner. Our MRI protocols consist of T1- and T2-weighted sequences (T1W, T2W) with TE=10–20 ms, TR=450–650 ms and TE=40 ms, TR = shortest respectively, with fat-saturated sequences and/or STIR, with a slice thickness 3 mm and a gap of 0.3 mm. Post-contrast images were utilized to characterize enhancement patterns within the tumors. In all cases of SCLs, a musculoskeletal pathologist confirmed the diagnosis. Demographic data of the patients was recorded including age, sex, and evidence of previous malignancy.

Two attending radiologists with at least 4 years of post-training experience retrospectively reviewed the imaging tests. The following imaging features were recorded: size and location of the lesion, margin and shape, presence or absence of intralesional calcification, and percentage of the lesion area containing fat. Additionally, areas of non-adipose content were carefully evaluated for signal characteristics and enhancement pattern.

Results

Among our 19 patients, more than three quarters ($n=15$, 79 %) were men, and the average age was 64.5 years old

(range, 40–80 years). Lesions in the posterior neck/upper back were found in seven cases (37 %) and four other lesions were localized in the shoulder ($n=4$, 21 %), overall reaching up to 60 % of cases (Fig. 1), and with all cases being men. The vast majority ($n=18$, 95 %) of the lesions were peripherally located, except for one mass that was found in the deep pelvis (Fig. 2). The majority of the lesions were confined to the subcutaneous fat ($n=14$, 74 %). Four lesions were entirely intramuscular in location (21 %), and one lesion (5 %) had mass effect on the muscle (Fig. 3). The average of the largest tumor dimension was 7.8 cm (range, 3.4–13 cm). Only two patients had a history of primary malignancy at the time of investigation of their subcutaneous mass. Two tumors were incidentally found on imaging, while the remaining 17 cases were identified on clinical exam.

All lesions had well-circumscribed borders with no adjacent fat stranding. A spiculated appearance or cystic components, characterized by internal fluid density, were not seen in any of the lesions. Only one lesion had peripheral well-defined calcification that was observed on CT scan. Tumor shape was predominantly ovoid ($n=16$, 84 %) or bi-lobed ($n=3$, 15.8 %). In all cases of SCLs, septations and/or non-adipose nodular areas were observed, with mass-like non-adipose components being much more common ($n=13$, 68 %) than linear septations ($n=6$, 32 %). Recognition of fat components and its differentiation from non-adipose components was easier on CT, MRI, or PET CT than on US (Figs. 1 and 3). Internal composition of the lesion was graded visually according to proportion of non-adipose and adipose components: no fat ($n=5$, 26 %), and 1–25 % ($n=3$, 16 %), 26–50 % ($n=4$, 21 %), 51–75 % ($n=2$, 11 %) and more than 75 % ($n=5$, 26 %) of fat.

In five of 19 cases, there was no intralesional macroscopic fat recognized on imaging. Another third of the cases ($n=7$) showed a relatively small amount of adipose content (less than 50 % of cross-sectional area of the lesion), while only the

Fig. 1 Spindle cell lipoma in the posterior neck/upper back. There is a well-defined mass predominantly composed of fat with hyperintense T1-weighted (T1W) signal (a) and loss of fat signal on short inversion recovery (STIR) sequence (b). There are linear hypointense T1W and hyperintense STIR septations (arrows) seen posteriorly within the mass, which enhance after contrast administration as seen on the fat-saturated post-contrast T1W image (c)

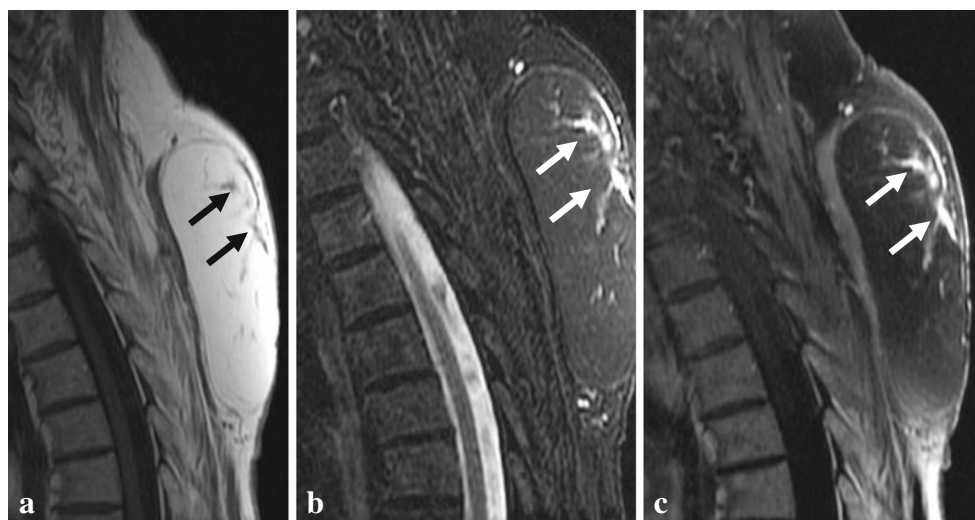




Fig. 2 Contrast-enhanced CT scan of the pelvis showing a heterogeneously enhancing ovoid mass in the deep low left aspect of the pelvis adjacent to the bladder and upper vagina with no discernible macroscopic fat. The pathology of this lesion proved to be a spindle cell lipoma

remaining one-third of lesions ($n=7$) revealed larger areas of fat (more than 50 %).

Various imaging features were noted in the non-adipose components (NACs) of SCLs. On ultrasound, the non-adipose-containing portions all revealed non-specific soft tissue echogenicity with moderate internal Doppler vascularity that was visually assessed. These areas on CT were hyperdense relative to normal fat and enhanced post-contrast administration with heterogeneous ($n=3$, 33.3 %), linear ($n=3$, 33.3 %), or homogeneous enhancement ($n=3$, 33.3 %). Three cases of spindle cell lipomas were imaged on PET-CT with increased uptake in the areas of non-adipose tissue (Fig. 4), with standardized uptake values (SUV) varying between 2 to 8.

On MRI, the NAC was isointense to skeletal muscle on T1-weighted (T1W) sequences, and of variable intermediate signal on T2-weighted (T2W) sequences. For the most part, these areas enhanced avidly post-gadolinium administration. In the 11 cases where MRI was performed (Table 1), homogeneous enhancement was seen in lesions almost entirely composed of soft tissue ($n=3$) (Fig. 4), but heterogeneous enhancement was noted in lesions consisting of a mixture of fat and non-adipose areas ($n=3$) (Fig. 3). Therefore, a relationship between

internal organization of a SCL and the pattern of enhancement of its NAC on MRI was noted such that the SCLs that contained more soft tissue and less fat enhanced more homogeneously post-contrast administration.

Ten of 19 cases had more than one cross-sectional imaging test. Despite this, a diagnosis of a SCL was not prospectively made in any of the cases, and a benign lipomatous lesion was suggested in only one case. In fat-containing SCLs, liposarcoma was proposed as the diagnosis in the final radiology report due to the pattern of enhancement of the non-adipose areas (avid, heterogeneous, or linear), size of the lesion, and relatively small fatty component. The second most commonly suggested diagnosis was that of a nerve sheath tumor. Myositis ossificans was suggested once in a case of a partially calcified SCL. Malignant tumors such as a sarcoma or metastases were suspected in all five cases of non-fat-containing SCLs.

Discussion

Spindle cell lipomas (SCL) were originally described by Enzinger and Harvey in 1975 [7] and they typically appear as well-circumscribed subcutaneous tumors in the posterior neck (Fig. 1), shoulder, or upper trunk of middle-aged men [8]. Up to 60 % of SCLs might be found in the aforementioned anatomical regions [9]. There have been reported cases of SCLs in the extremities, oral cavity, larynx, bronchus, esophagus, orbit, scalp, breast, and ischiorectal fossa [10]. SCLs present predominantly in male patients (79 % in our series and up to the 90 % reported in the literature [10]). It has been postulated that the male predominance can be explained by the expression of androgen receptors by SCLs [11]. Usually SCLs are small in size (2–5 cm) and can grow above 10 cm [9]. Some patients have multiple lesions and familial occurrence has been reported, mostly in men [12]. Spindle cell lipomas typically present as slowly growing masses, which presumably never recur after local excision [3, 4].

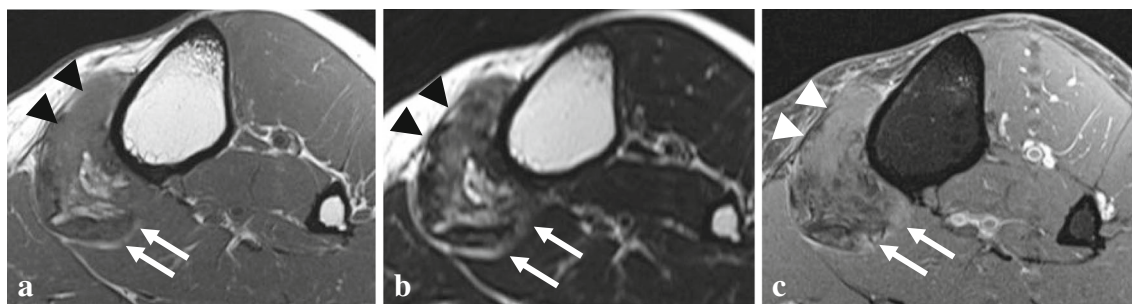


Fig. 3 MRI of a spindle cell lipoma consisting of mixed areas of macroscopic fat (arrows) and areas of non-adipose tissue (arrowheads) abutting the medial portion of the left soleus muscle. The anterior non-adipose portion of the lesion is isointense on T1 (a), of variable

intermediate signal on T2 (b), and faintly homogeneously enhances after contrast administration on the T1 fat-suppressed post-contrast image (c). Linear striated heterogeneous enhancement is seen in the posterior part of the lesion (white arrow in a–c) owing to areas of fat and soft tissue

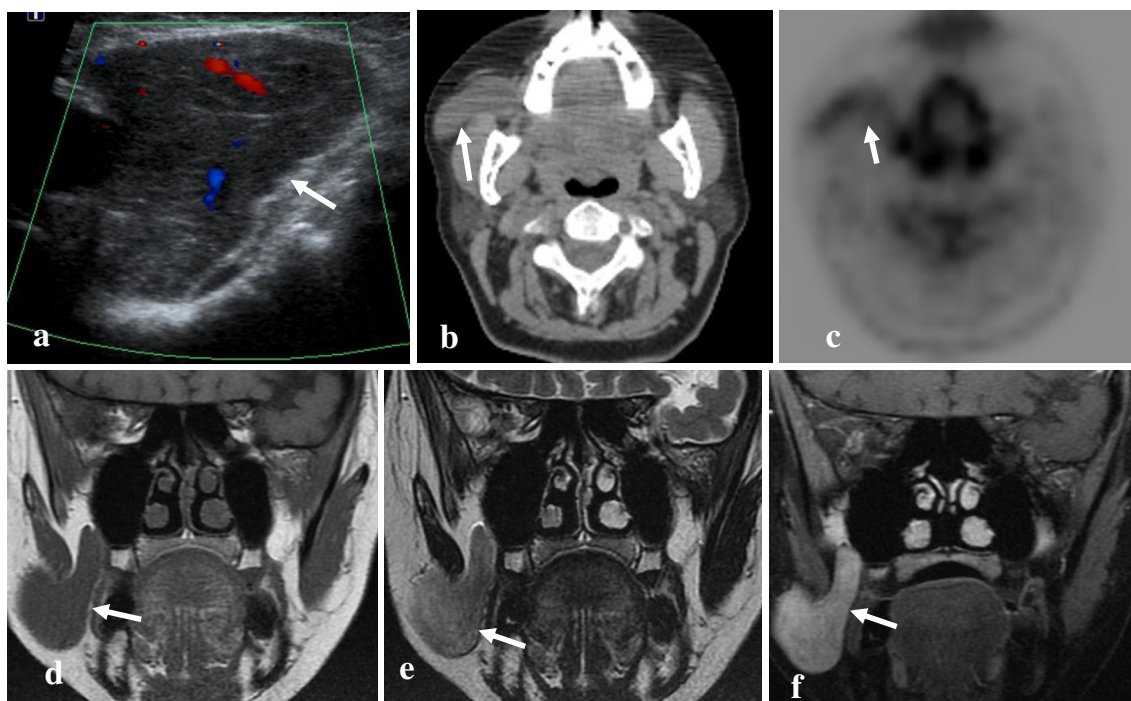


Fig. 4 Spindle cell lipoma (*arrows*) presenting as a slowly growing hypoechoic mass relative to normal fat in the right cheek with internal Doppler vascularity on ultrasound (a). PET CT scan demonstrates that the lesion is hyperdense relative to normal fat and has increased metabolic

uptake on PET CT (b, c). On coronal MR images, the mass reveals hypointense T1W signal (d) and heterogeneous intermediate T2W signal (e), and homogeneous enhancement post-contrast administration (f)

SCLs are composed of varying proportions of mature fat cells, small and uniform spindle cells, and eosinophilic collagen bundles [13]. The spectrum of these lesions originating from fat varies from tumors that resemble ordinary lipomas with narrow streaks of spindle cells to neoplasms that are mostly composed of spindle cells with just a few fat cells [9], occasionally posing a great challenge in diagnosing the lesion as a lipoma.

Histologically, bland fibroblast-like spindle cells are arranged in characteristic parallel arrays (“school of fish”) with highly variable amounts of mature adipocytes on a background of “ropelike” collagen bundles, myxoid stroma, mast cells, and blood vessels (Fig. 5) [14]. On immunohistochemistry, the spindle cells are CD34-positive and they are negative for S-100 protein, which helps to distinguish them from nerve sheath tumors. Spindle cell lipomas can exhibit 13q and/or

16q chromosomal deletions that are considered characteristic for this family of lipomas [15].

Classically, lipomas show no cellular atypia and lack fibrous septae, both of which are features of atypical lipomatous tumor/well-differentiated liposarcoma. In occasional cases, distinction of these lesions may be challenging histologically, ultimately requiring extensive sampling of the excision specimen [16].

There are several histological subtypes of spindle cell lipomas. A pleomorphic lipoma is a histological variant with nuclear pleomorphism and occasional nuclear atypia resembling atypical lipomas [17]. Intramuscular spindle cell lipomas may demonstrate a well-circumscribed appearance or infiltrate the skeletal muscle (Fig. 3), completely replacing the muscle bundles in some cases [18, 19]. Traversing muscle fibers might result in a striated appearance, which is not typically seen with other lipomas [20] (Fig. 3). A dermal

Table 1 Characteristics of non-adipose components (NAC) in spindle cell lipomas in 11 cases imaged on MRI

Grade of NAC	N cases	Internal organization	T1W signal	T2W signal	Enhancement
No fat	2	Homogeneous mass	Low	Intermediate to high	Avid, homogeneous
1–25 %	3	Mass with fatty septations			Homogeneous or heterogeneous
26–50 %	2	Heterogeneous mass			Homogeneous or heterogeneous
51–75 %	1	Heterogeneous mass			Heterogeneous
>75 %	3	Fatty mass with thin non-adipose septa			Linear

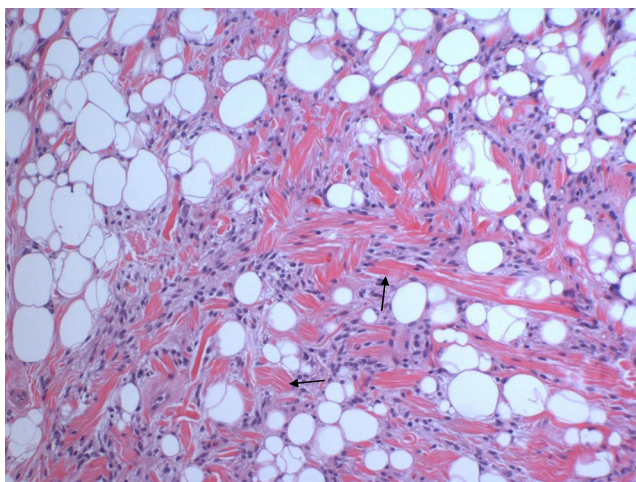


Fig. 5 Photomicrograph of histopathologic specimen of spindle cell lipoma demonstrates bland spindle-shaped cells arranged in parallel arrays (*arrows*) with scattered vascular spaces and ropey collagen bundles, admixed with mast cells. The adipocytes are benign but of variable sizes. The spindle cells were reactive to CD34 staining (not shown), supporting the diagnosis. S100 staining was negative, further excluding the diagnosis of a peripheral nerve sheath tumor (H&E 100 \times)

variant of a spindle cell lipoma can be seen in women, presenting as a poorly circumscribed nodule with myxoid stroma that can occasionally displace adnexal structures (Fig. 2) [21]. Several other morphological subtypes of spindle cell lipomas have been described, including angiomatous and myxoid stroma variants, based on the predominant histological component [22–24].

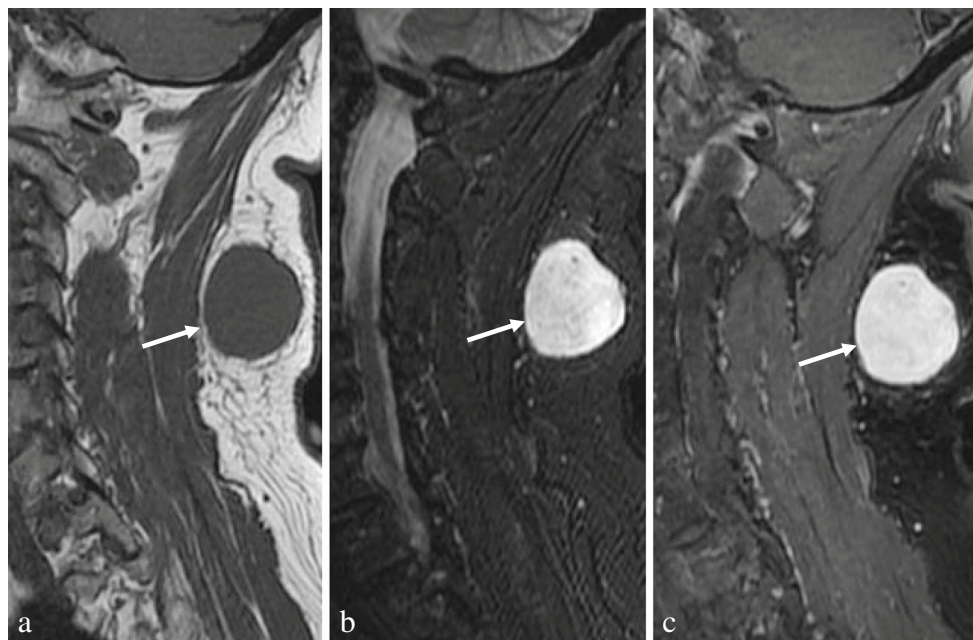
“Low-fat” and “fat-free” variants may be challenging to diagnose even pathologically (Figs. 4 and 6). Five of the 19 cases in our series were devoid of fat on imaging. Similar to these results, almost no fat was seen

histologically in 10 % of cases in a retrospective histological review of 300 cases of spindle cell lipomas at the Cleveland Clinic [14]. The key to suggesting the diagnosis lies in the typical location of the lesion, the patient’s demographic characteristics that are supported by imaging features [14]. Awareness of these variants will help the pathologist to diagnose spindle cell lipoma by appreciating the typical histology (i.e., bland spindle cells, ropey collagen, mast cells, and myxoid stroma) and immunohistochemical properties (expression to CD34) of the spindle cell component despite the absence of an easily recognizable adipocytic component.

The imaging features of spindle cell lipoma have not been well documented in the literature, as they are often excised without imaging due to their typical small size and superficial location. Only one study by Bancroft et al. [4] reported the computed tomography (CT), or magnetic resonance imaging (MRI) appearance of spindle cell lipomas in nine patients with particular attention to its non-fatty component. Comparable to our results, this study reported a variable amount of fat in combination with soft tissue septations or nodular areas in these lesions.

In our practice, non-adipose components of SCLs were isointense to skeletal muscle on T1-weighted imaging (T1W) and of variable signal compared to fat on T2-weighted (T2W) sequences. In agreement with Bancroft et al. [4], our cases of SCLs with non-adipose components displayed enhancement of the non-fat-containing areas after contrast administration. We propose that the type of enhancement is related to the internal organization of the lesion such that lesions with multiple soft tissue septations or non-adipose nodularity have heterogeneous enhancement, while lesions

Fig. 6 MRI of the cervical spine in a patient with a spindle cell lipoma (*arrows*) reveals a well-defined homogeneous mass in the subcutaneous tissues of the posterior neck in a 68-year-old man. The mass has no discernible fat on the sagittal T1W fast spin echo (a) or on the sagittal STIR images (b). After contrast administration (c), there is avid enhancement of the lesion. Although the demographic characteristics and location are typical for a spindle cell lipoma, the imaging features in this case makes it extremely challenging to diagnose a lipomatous tumor. Final pathological analysis confirmed the low-fat variant of spindle cell lipoma with some myxoid change in the stroma



that contain no fat demonstrate homogeneous enhancement. In accordance with that of Choi et al. [25], enhancement was more pronounced on post-contrast MRI compared to CT scans, reflecting the higher sensitivity and greater dynamic range of MRI to detect changes after contrast enhancement.

Increased metabolic activity on positron emission tomography CT (PET-CT) was seen in all three of our cases, which were imaged by PET-CT. There has been no study in the English literature describing the metabolic activity expected in SCLs; yet, increased metabolic uptake has been reported in desmoid fibromatosis [26] and in a spindle cell neoplasm of the parotid gland [27].

The diagnostic challenge of spindle cell lipomas lies in their differentiation from other soft-tissue tumors. The differential diagnosis for a spindle cell lipoma includes a liposarcoma, a schwannoma, and a neurofibroma. Features that suggest malignancy in a lipomatous tumor are increased patient age, large size (>10 cm), fat stranding, intralesional fat content less than 75 %, presence of thick septations, and nodular or globular non-adipose areas [28]. The age, size criteria, nodular shape of non-adipose component, as well as relatively little fat content of a liposarcoma overlap with the features of spindle cell lipomas in our experience; however, none of the spindle cell lipomas in our study were associated with fat stranding. Moreover, liposarcomas are typically located in the deep soft tissues of the extremities and in the retroperitoneum, whereas spindle cell lipomas are generally found in the subcutaneous layers of the head and neck, upper back, and shoulder region.

A schwannoma of a cutaneous nerve is often considered as a differential possibility for SCLs, as it presents as a slowly growing well-circumscribed solitary mass of the deep or superficial soft tissues. MRI signal characteristics of schwannomas overlap with that of spindle cell lipomas due to their low signal intensity on T1W images and avid enhancement post-gadolinium administration [2]. One differentiating imaging feature is that in general, schwannomas are hyperintense on T2W images, while spindle cell lipomas are intermediate in signal on T2W images.

A preoperative diagnosis of spindle cell lipoma is crucial to surgical management, as it impacts the surgical approach, duration of the procedure, and extent of surgery with concern for neurovascular injury and increased morbidity in the post-operative period [16]. As discussed earlier, there is an overlap between the imaging features of SCLs and more aggressive entities such as liposarcomas, and the differential diagnosis would therefore include both entities in many cases. However, if a SCL is included in the differential possibilities, we advocate image-guided tissue biopsy over a surgical biopsy prior to surgical management [16, 29].

A few factors limited the number of SCL imaging cases that were available for review. Firstly, many subcutaneous

lipomas are usually removed surgically without imaging, which limits the quantity of cases with pre-operative imaging that could have been reviewed. Secondly, histopathologic classification of these lesions may be suboptimal, particularly with biopsy material, as a close resemblance between extramammary myofibroblastoma, pleomorphic lipoma, and spindle cell lipoma is well recognized by pathologists such that some excised lesions could have been classified under these alternate diagnoses, particularly in the case of myofibroblastoma where sufficient sampling was not undertaken to identify a fatty component and the clinical findings were not clear [30–34].

In summary, the finding of a well-circumscribed non-aggressive subcutaneous mass located in the head and neck region in a middle-aged male patient should raise the suspicion of a lipoma or a lipoma variant such as spindle cell lipoma regardless of fat content. Due to the overlap of radiological findings of SCLs with other soft tissue tumors including a well-differentiated liposarcoma, confirmation of the pathology of this lesion is still recommended with biopsy, followed by surgical excision. The US, CT, PET CT, and MRI imaging characteristics of spindle cell lipomas detailed above can help the radiologist prospectively suggest this diagnosis prior to biopsy or excision to help the clinician avoid unnecessary radical surgery.

Acknowledgments The authors would like to thank Dr. Raquel del Carpio-O'Donovan, M.D., FRCPC, Professor of Radiology at the McGill University Health Center (MUHC) and Dr. Huy Le, M.D., FRCPC, Assistant Professor of Radiology at the Jewish General Hospital for their comments and support in preparing the manuscript.

Conflicts of interest The authors declare that they have no conflicts of interest.

References

1. Choia Y, Leea I, Kimb S, et al. Analyses of short-term follow-up MRI and PET-CT for evaluation of residual tumour after inadequate primary resection of malignant soft-tissue tumours. *Clin Radiol*. 2013;68:117–24.
2. Beaman FD, Kransdorf MJ, Andrews TR, Murphey MD, Arcara LK, Keeling JH. Superficial soft-tissue masses: analysis, diagnosis, and differential considerations. *Radiographics*. 2007;27:509–23.
3. Murphey MD, Carroll JF, Flemming DJ, Pope TL, Gannon FH, Kransdorf MJ. From the archives of the AFIP: benign musculoskeletal lipomatous lesions. *Radiographics*. 2004;24:1433–66.
4. Bancroft LW, Kransdorf MJ, Peterson JJ, O'Connor MI. Benign fatty tumors: classification, clinical course, imaging appearance, and treatment. *Skelet Radiol*. 2006;35:719–33.
5. Bui-Mansfield LT, Kaplan KJ. Spindle cell lipoma of the upper back. *AJR*. 2002;179:1158.
6. Mandal RV, Duncan LM, Austen Jr WG, Nielsen GP. Infiltrating intramuscular spindle cell lipoma of the face. *J Cutan Pathol*. 2009;36:70–3.

7. Enzinger FM, Harvey DA. Spindle cell lipoma. *Cancer*. 1975;36:1852–9.
8. Rydholm A, Berg NO. Size, site and clinical incidence of lipoma. Factors in the differential diagnosis of lipoma and sarcoma. *Acta Orthop Scand*. 1983;54:929–34.
9. Miettinen M. *Modern soft tissue pathology: tumors and non-neoplastic conditions*. New York: Cambridge University Press; 2010.
10. Bancroft LW, Kransdorf MJ, Peterson JJ, Sundaram M, Murphey MD, O'Connor MI. Imaging characteristics of spindle cell lipoma. *AJR Am J Roentgenol*. 2003;181:1251–4.
11. Syed S, Martin AM, Haupt H, Podolski V, Brooks JJ. Frequent detection of androgen receptors in spindle cell lipomas: an explanation for this lesion's male predominance? *Arch Pathol Lab Med*. 2008;132:81–3.
12. Fanburg-Smith JC, Devaney KO, Miettinen M, Weiss SW. Multiple spindle cell lipomas: a report of 7 familial and 11 nonfamilial cases. *Am J Surg Pathol*. 1998;22:40–8.
13. Fletcher CD, Martin-Bates E. Spindle cell lipoma: a clinicopathological study with some original observations. *Histopathology*. 1987;11:803–17.
14. Billings SD, Folpe AL. Diagnostically challenging spindle cell lipomas: a report of 34 "low-fat" and "fat-free" variants. *Am J Dermatopathol*. 2007;29:437–42.
15. Thompson LD. Spindle-cell lipoma. *Ear Nose Throat J*. 2009;88:992–3.
16. Olaleye O, Moorthy BR, Lawson C, Black M, Mitchell D. Left supraclavicular spindle cell lipoma. *Int J Otolaryngol*. 2010;2010:942–52.
17. Shmookler BM, Enzinger FM. Pleomorphic lipoma: a benign tumor simulating liposarcoma. A clinicopathologic analysis of 48 cases. *Cancer*. 1981;47:126–33.
18. Fletcher CD, Martin-Bates E. Intramuscular and intermuscular lipoma: neglected diagnoses. *Histopathology*. 1988;12:275–87.
19. Salvatorea C, Antonioa B, Del Vecchioa W, Lanzaa A, Tartaroa GP, Giuseppa C. Giant infiltrating lipoma of the face: CT and MR imaging findings. *AJNR*. 2003;24:283–6.
20. Matsumoto K, Hukuda S, Ishizawa M, Chano T, Okabe H. MRI findings in intramuscular lipomas. *Skelet Radiol*. 1999;28:145–52.
21. Zelger BW, Zelger BG, Plörer A, Steiner H, Fritsch PO. Dermal spindle cell lipoma: plexiform and nodular variants. *Histopathology*. 1995;27:533.
22. Zamecnik M, Michal M. Angiomatous spindle cell lipoma: report of three cases with immunohistochemical and ultrastructural study and reappraisal of former 'pseudoangiomatous' variant. *Pathol Int*. 2007;57:26.
23. Diaz-Cascajo F, Borghi S, Weyers W. Fibrous spindle cell lipoma: report of a new variant. *Am J Dermatopathol*. 2001;23:112.
24. Suster S, Fisher C, Moran CA. Dendritic fibromyxolipoma: clinicopathologic study of a distinctive benign soft tissue lesion that may be mistaken for a sarcoma. *Ann Diagn Pathol*. 1998;2:111.
25. Choi JW, Kim HJ, Kim J, Kim HJ, Cha JH, Kim ST. Spindle cell lipoma of the head and neck: CT and MR imaging findings. *Neuroradiology*. 2013;55:101–6.
26. Souza FF, Fennessy FM, Yang Q, Van den Abbeele AD. PET/CT appearance of desmoid tumour of the chest wall. *Br J Radiol*. 2010;83:e39–42.
27. Kiendys U, Ham H, Bauters W, Van den Broecke C, Deron P, Goethals I. F-18 fluorodeoxyglucose (FDG) positron emission tomography (PET)-positive parotid incidentaloma: prevalence and clinical significance. *Rep Med Imaging*. 2009;2:1–6.
28. Kransdorf MJ, Bancroft LW, Peterson JJ, Murphey MD, Foster WC, Temple HT. Imaging of fatty tumors: distinction of lipoma and well-differentiated liposarcoma. *Radiology*. 2002;224:99–104.
29. Brisson M, Kashima T, Delaney D, et al. MRI characteristics of lipoma and atypical lipomatous tumor/well-differentiated liposarcoma: retrospective comparison with histology and MDM2 gene amplification. *Skelet Radiol*. 2013;42:635–47.
30. Maggiani F, Debiec-Rychter M, Verbeeck G, Sciort R. Extramammary myofibroblastoma is genetically related to spindle cell lipoma. *Virchows Arch*. 2006;449:244–7.
31. McMenamin ME, Fletcher CD. Mammary-type myofibroblastoma of soft tissue: a tumor closely related to spindle cell lipoma. *Am J Surg Pathol*. 2001;25:1022–9.
32. Hox V, Vander Poorten V, Delaere PR, Hermans R, Debiec-Rychter M, Sciort R. Extramammary myofibroblastoma in the head and neck region. *Head Neck*. 2009;31:1240–4.
33. Chen BJ, Mariño-Enríquez A, Fletcher CD, Hornick JL. Loss of retinoblastoma protein expression in spindle cell/pleomorphic lipomas and cytogenetically related tumors: an immunohistochemical study with diagnostic implications. *Am J Surg Pathol*. 2012;36:1119–28.
34. Flucke U, van Krieken JH, Mentzel T. Cellular angiofibroma: analysis of 25 cases emphasizing its relationship to spindle cell lipoma and mammary-type myofibroblastoma. *Mod Pathol*. 2011;24:82–9.